Supporting Information

Uniphase Ruthenium-Iridium Alloy-Based Electronic Regulation for Electronic Structure-Function Study on Methane Oxidation to Methanol

Le Yang [1], Jinxu Huang [1], Sheng Dai [2], Xuan Tang [2], Zhe Hu [1], Ming Li [3], Hui Zeng[1*], Rafael Luque [4, 5], Peigao Duan[6], Zebao Rui[1*]

[1] *School of Chemical Engineering and Technology, Guangdong Engineering Technology Research Center for Platform Chemicals from Marine Biomass and Their Functionalization, Sun Yat-sen University, Zhuhai 519082, China*

[2] *Key Laboratory for Advanced Materials and Feringa Nobel Prize Scientist Joint Research Center, School of Chemistry & Molecular Engineering, East China University of Science and Technology, Shanghai 200237, P.R. China*

[3] *Polymer Program, Institute of Materials Science, University of Connecticut, Storrs, CT, 06269, USA*

[4]*Departamento de Química Orgánica, Universidad de Córdoba, Campus de Rabanales, Edificio Marie Curie (C-3), Ctra Nnal IV-A, Km 396, E14014, Cordoba, Spain.*

[5]*Peoples Friendship University of Russia (RUDN University), 6 Miklukho-Maklaya Str.,117198, Moscow, Russia.*

[6]*Shaanxi Key Laboratory of Energy Chemical Process Intensification, School of Chemical Engineering and Technology, Xi'an Jiaotong University, No. 28, West Xianning Road, Xi'an, Shaanxi 710049, PR China.*

*Corresponding author, Email address: ruizebao@mail.sysu.edu.cn (Z.B. Rui), zenghui5@mail.sysu.edu.cn (H. Zeng)

Experiments

Synthesis of Ru_xIr_{1-x} NPs (x=0, 0.3, 0.5, 0.7)

Ru_xIr_{1-x} NPs (x=0, 0.3, 0.5, 0.7) were prepared by a polyol process. In a typical procedure, appropriate amounts of $H_2IrCl_6.6H_2O$ and/or $RuCl_3.3H_2O$ with corresponding Ru:Ir atom ratios of 3:7, 5:5, 7:3 and 0:1 were dissolved in 20 mL ethylene glycol (EG), where 0.05 g PVP (k30) was added. Then the solution was heated to 150 ^oC with a reflux condenser for 30 min. The resulting deep yellow/gray mixture was removed from the heat. After the mixture was cooled to room temperature, the NPs were collected by centrifugation at 14,000 rpm for 20 min, washed by methanol for several times, and finally dispersed in methanol.

Synthesis of Ru_xIr_{1-x}@Cu-BTC

In a typical procedure, 0.002 g Ru_xIr_{1-x} NPs and 0.8 g PVP (k-30) were dissolved in 40 mL methanol solution of trimesic acid (3.5 g) to form mixture A. Then a 40 mL methanol solution of $Cu(NO_3)_2.3H_2O$ (7.28 g) was added into mixture A to form mixture B, which was kept stirring for 5 min before settling at room temperature for 3.5 h without stirring. The product was collected by centrifugation, washed several times with methanol, and dried at 60 ^oC overnight.

Synthesis of $Ru_xIr_{1-x}O_2$/CuO

The obtained $Ru_xIr_{1-x}O_2$@Cu-BTC was treated in air with a heating rate of 5 ^oC/min from room temperature to 500 ^oC and held for 2 h, to achieve target products, $Ru_xIr_{1-x}O_2$/CuO. 1 g Ru_xIr_{1-x}@Cu-BTC approximately derived 0.2 g $Ru_xIr_{1-x}O_2$/CuO, and Ru_xIr_{1-x} weight faction kept 1% theoretically.

Characterization technique

The field emission scanning electron microscope (SEM) images were performed using a Hitachi S-4800 SEM. Transmission electron microscope (TEM) imaging was carried out on a JEM-2010F and ThermoFisher Talos F200X field emission electron microscope at an acceleration voltage of 200 kV. Powder X-ray diffraction (PXRD) patterns were collected over the 2theta range of 5-80^{o} at room temperature with a Philips PW3040/60 automated diffractometer using monochromated Cu-Kα radiation (λ= 1.5418 Å). Diffraction patterns were collected at a scanning rate of 10°/min. The surface electronic states were investigated by X-ray photoelectron spectroscopy (XPS, Thermo VG ESCALAB250 using Al Kα radiation). The XPS data were internally calibrated, fixing the binding energy of C 1s at 284.6 eV. CH_4-temperature programmed reduction (CH_4-TPR) experiments were conducted on a chemisorption apparatus (Micromeritics Autochem 2920) connected with an online mass spectrometer (HIDEN QIC 20) to analyze the effluent gas. 100 mg of catalyst was placed in a U-shaped quartz tube and heated at a rate of 10 °C /min in a flow of 5% CH_4/He mixture with a flow rate of 30 mL/min. Before measurement, the catalyst was first heated to 200 °C in He for 30 min to remove the surface adsorbates.

Catalytic activity tests

Typically, 10 mg catalyst and 30 mL DI water was loaded in a 100 mL reactor with PTFE lining (Anhui Kemi Machinery Technology Co., Ltd., Anhui, China; Model MS100-P5-T4-HC1-SV. All parts of the autoclave that directly contacted the reactants were made of Hastelloy). Batch reactor-tests were conducted at a fixed methane pressure of 3 bar with 1 bar air unless otherwise specified. Reactions were carried out at 150 ^{o}C for 3 h. After the reaction, the reactor cooled to room temperature naturally and the liquid product was filtrated through a 0.22 μm filter using a syringe before

collected in a GC vial for further analysis. For the catalytic recycle test, the catalyst was collected by centrifugation and dried at 80^{o}C before tested for the next run. Because there was mass loss when collecting the catalyst, the catalyst was weighed every time before added into the reactor.

Product analysis

Identification analysis was performed using two approaches. First, we used a Bruker 600 MHz ^{1}H-NMR and ^{13}C-NMR to identify the products. The main product is methanol, and side products consist of ethanol, formaldehyde and acetaldehyde. We further compare the GC signal against model compounds, methanol ethanol, formaldehyde and acetaldehyde, to double check the product identity. Quantitative analysis was performed using a Shimadzu GC-2030 equipped with a 50 m × 0.2 mm × 0.33 μm HP-5 capillary column, a flame ionization detector (FID), and an A0C-20i autoinjector. The injection port temperature was 200 °C, and the column temperature program consisted of a 3 min soak at 30 ^{o}C followed by a 5 ^{o}C /min ramp to 100 ^{o}C. External standard method was used for the quantification.

In this work, each single datum point was measured by repeating three times under the same condition. Methanol yield was calculated using an external standard method, while the unidentified product was calculated using the same correction factor as methanol. Selectivity was calculated as (peak area of CH_3OH)/(total peak areas of the liquid products)×100%.

Computational Details

All the DFT calculations were performed by CASTEP code implemented in Materials Studio software. The generalized gradient approximation (GGA) with the Perdew-Burke-Ernzerhof PBE functional and ultrasoft pseudo potential were employed for the periodic plane-wave approach. Self-consistent field (SCF) tolerance in the

structural optimizations was set to be 2.0×10^{-6} eV/atom, and the energy cutoff used was 400 eV. A 2×2×1 grid of k-points was used to sample the Brillouin zone. Tkatchenko-Scheffler (TS) dispersion correction has been used to account for the van der Waals energies. Three crystal structures (RuO_2, IrO_2, CuO) were obtained from the crystal database of Materials Project website. The surface of MO_2/CuO (M=Ir, Ru) is composed of a monolayer of MO_2 (1, 1, 0) and three CuO (1, 0, 0) layers. In addition, the thickness of the vacuum layer is 15 Å to avoid the interaction between the adjacent upper and lower surfaces. In the process of structural optimization, the bottom two CuO (1, 0, 0) layers are fixed. Half of Ru atoms in the optimized RuO_2/CuO surface were substituted with Ir atoms was further optimized for constructing the $Ru_{0.5}Ir_{0.5}O_2$/CuO surface.

Table S1. XPS data of Ru_xIr_{1-x} (x=0.3, 0.5, 0.7) NPs.

	% Atom from XPS			Theoretical Ru/Ir Atomic ratio
	Ru	Ir	Ru/Ir	
$Ru_{0.7}Ir_{0.3}$	2.97	1.43	2.08	2.33
$Ru_{0.5}Ir_{0.5}$	1.15	1.16	0.99	1
$Ru_{0.3}Ir_{0.7}$	2.42	5.92	0.41	0.43

Table S2. Atomic charges on the samples.

IrO_2/CuO								
Species	Ion	s	p	d	f	Total	Charge (e)	Spin (hbar/2)
O	1	1.91	4.6	0	0	6.51	-0.51	0.12
O	2	1.89	4.78	0	0	6.67	-0.67	0.11
O	3	1.88	4.73	0	0	6.62	-0.62	0.21
O	4	1.87	4.82	0	0	6.69	-0.69	0.06
O	5	1.9	4.62	0	0	6.52	-0.52	0.01
O	6	1.89	4.78	0	0	6.67	-0.67	0.11
O	7	1.88	4.73	0	0	6.62	-0.62	0.21
O	8	1.87	4.82	0	0	6.69	-0.69	0.06
O	9	1.9	4.62	0	0	6.52	-0.52	0.01
O	10	1.87	4.73	0	0	6.6	-0.6	0.03
Cu	1	0.54	0.37	9.4	0	10.31	0.69	0.35
Cu	2	0.54	0.37	9.44	0	10.34	0.66	-0.28
Cu	3	0.45	0.34	9.5	0	10.29	0.71	0.09
Cu	4	0.54	0.25	9.27	0	10.06	0.94	0.08
Cu	5	0.56	0.38	9.43	0	10.37	0.63	0.34
Cu	6	0.55	0.28	9.39	0	10.22	0.78	0.28
Ir	1	2.62	6.42	7.13	14	30.17	0.83	0.01
Ir	2	2.62	6.45	7.08	14	30.15	0.85	0.29

$Ir_{0.5}Ru_{0.5}O_2/CuO$								
Species	Ion	s	p	d	f	Total	Charge (e)	Spin (hbar/2)
O	1	1.91	4.6	0	0	6.51	-0.51	0.23
O	2	1.89	4.78	0	0	6.67	-0.67	0.11
O	3	1.88	4.74	0	0	6.62	-0.62	0.22
O	4	1.87	4.82	0	0	6.69	-0.69	0.07
O	5	1.88	4.65	0	0	6.53	-0.53	0.02
O	6	1.89	4.78	0	0	6.67	-0.67	0.11
O	7	1.88	4.74	0	0	6.62	-0.62	0.22
O	8	1.87	4.82	0	0	6.69	-0.69	0.07
O	9	1.88	4.65	0	0	6.53	-0.53	0.02
O	10	1.88	4.71	0	0	6.59	-0.59	0.02
Cu	1	0.54	0.37	9.4	0	10.31	0.69	0.35
Cu	2	0.54	0.37	9.44	0	10.34	0.66	-0.29
Cu	3	0.46	0.37	9.53	0	10.36	0.64	0.08
Cu	4	0.54	0.25	9.27	0	10.07	0.93	0.08
Cu	5	0.56	0.38	9.43	0	10.37	0.63	0.37
Cu	6	0.55	0.28	9.39	0	10.22	0.78	0.29
Ru	1	2.36	6.21	6.38	0	14.95	1.05	0.09
Ir	1	2.63	6.49	7.15	14	30.28	0.72	0.48

RuO_2/CuO								
Species	Ion	s	p	d	f	Total	Charge (e)	Spin (hbar/2)
O	1	1.88	4.64	0	0	6.52	-0.52	-0.01
O	2	1.88	4.79	0	0	6.67	-0.67	0.1
O	3	1.87	4.77	0	0	6.64	-0.64	0.2
O	4	1.87	4.77	0	0	6.65	-0.65	0.08
O	5	1.86	4.7	0	0	6.56	-0.56	0
O	6	1.88	4.79	0	0	6.67	-0.67	0.1
O	7	1.87	4.77	0	0	6.64	-0.64	0.2
O	8	1.87	4.77	0	0	6.65	-0.65	0.08
O	9	1.86	4.7	0	0	6.56	-0.56	0
O	10	1.87	4.7	0	0	6.57	-0.57	0.04
Cu	1	0.53	0.36	9.36	0	10.26	0.74	0.13
Cu	2	0.54	0.38	9.39	0	10.31	0.69	-0.24
Cu	3	0.47	0.38	9.55	0	10.4	0.6	0.07
Cu	4	0.53	0.25	9.29	0	10.08	0.92	0.14
Cu	5	0.55	0.37	9.41	0	10.33	0.67	0.41
Cu	6	0.53	0.4	9.34	0	10.27	0.73	0.34
Ru	1	2.33	6.15	6.51	0	14.99	1.01	0.13
Ru	2	2.36	6.38	6.48	0	15.22	0.78	-0.07

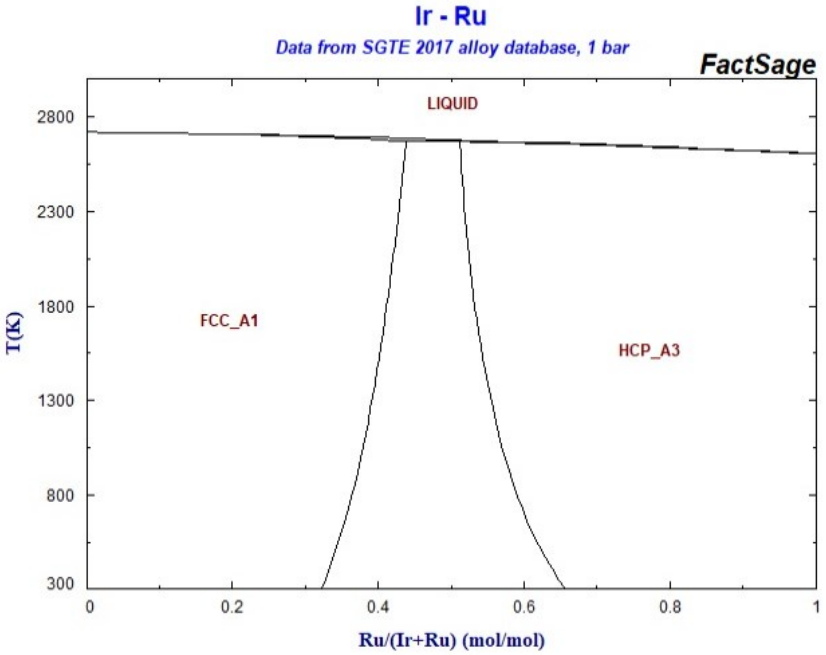

Figure S1. RuIr alloy phase diagram.
(http://www.crct.polymtl.ca/FACT/documentation/#opennewwindow)

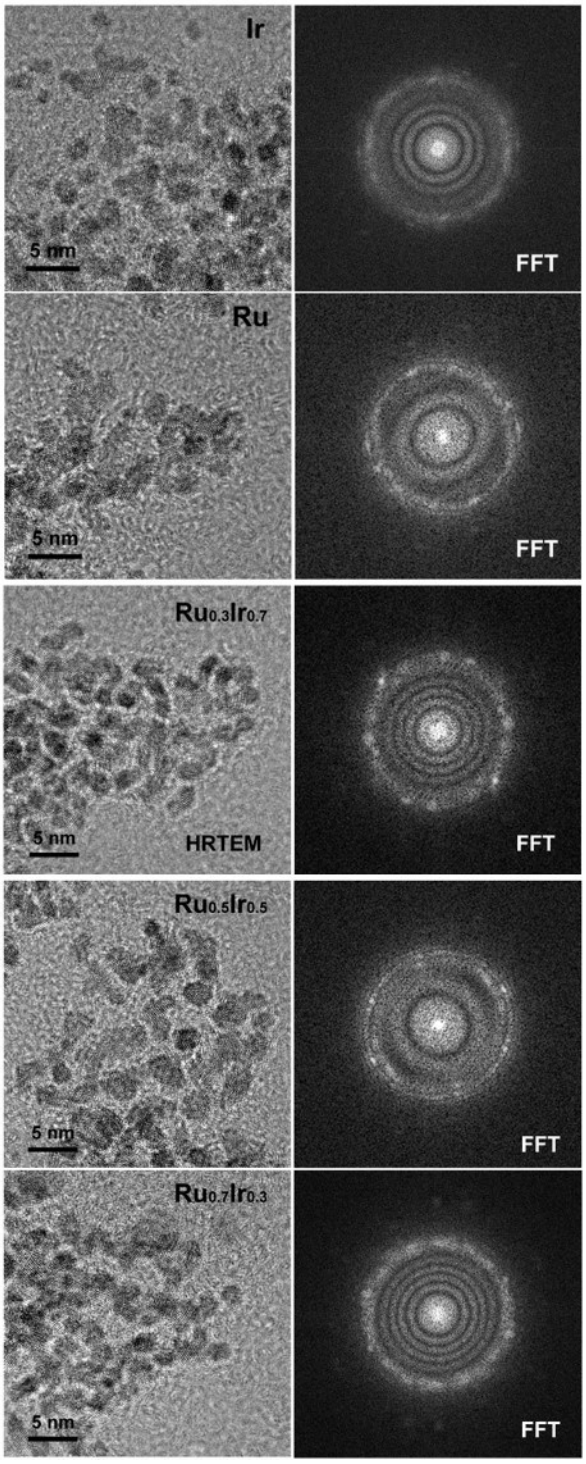

Figure S2. HRTEM images and corresponding FFT patterns of the NPs.

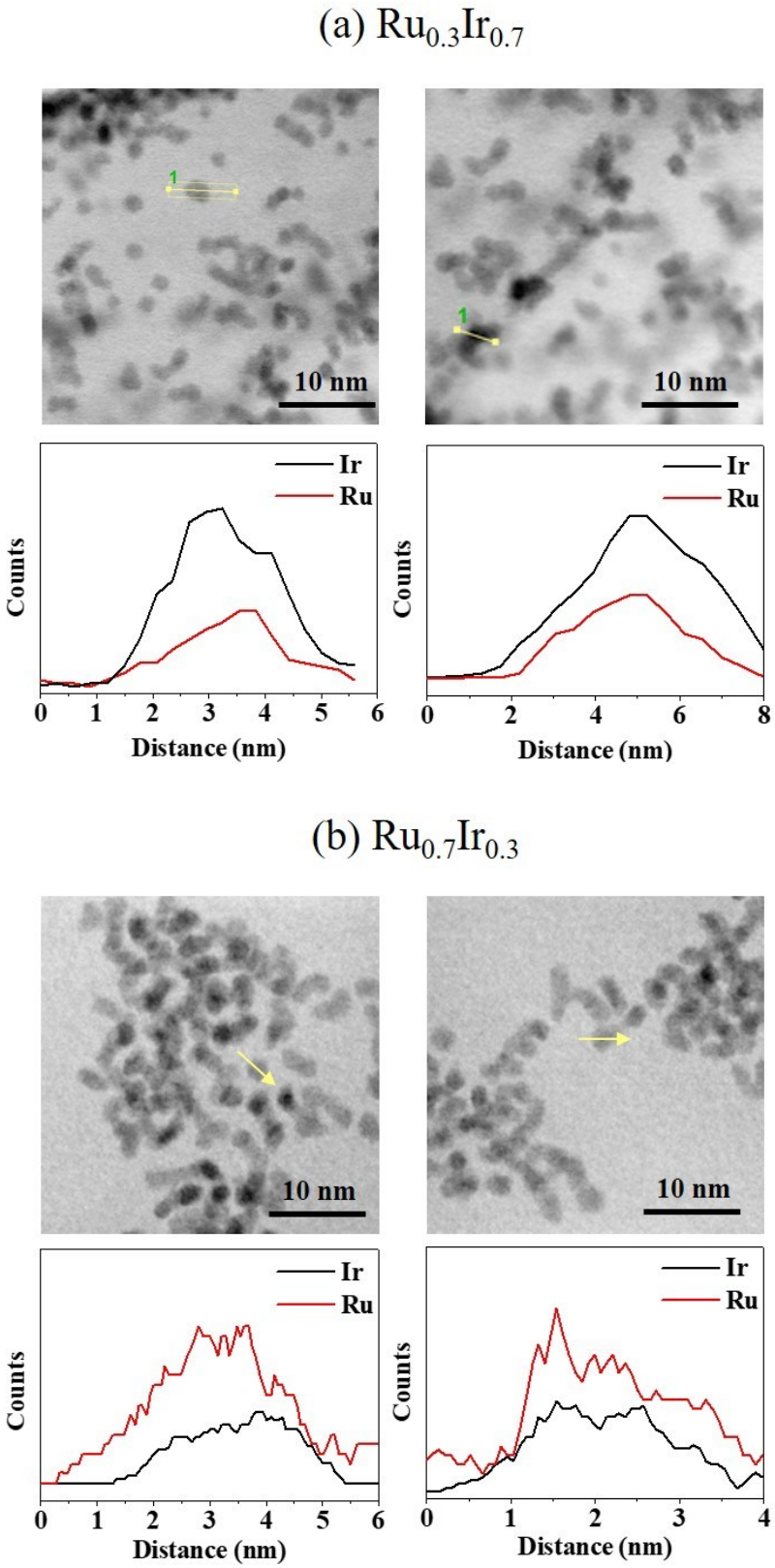

Figure S3. TEM and line-scan of (a) $Ru_{0.3}Ir_{0.7}$ and (b) $Ru_{0.7}Ir_{0.3}$ NPs.

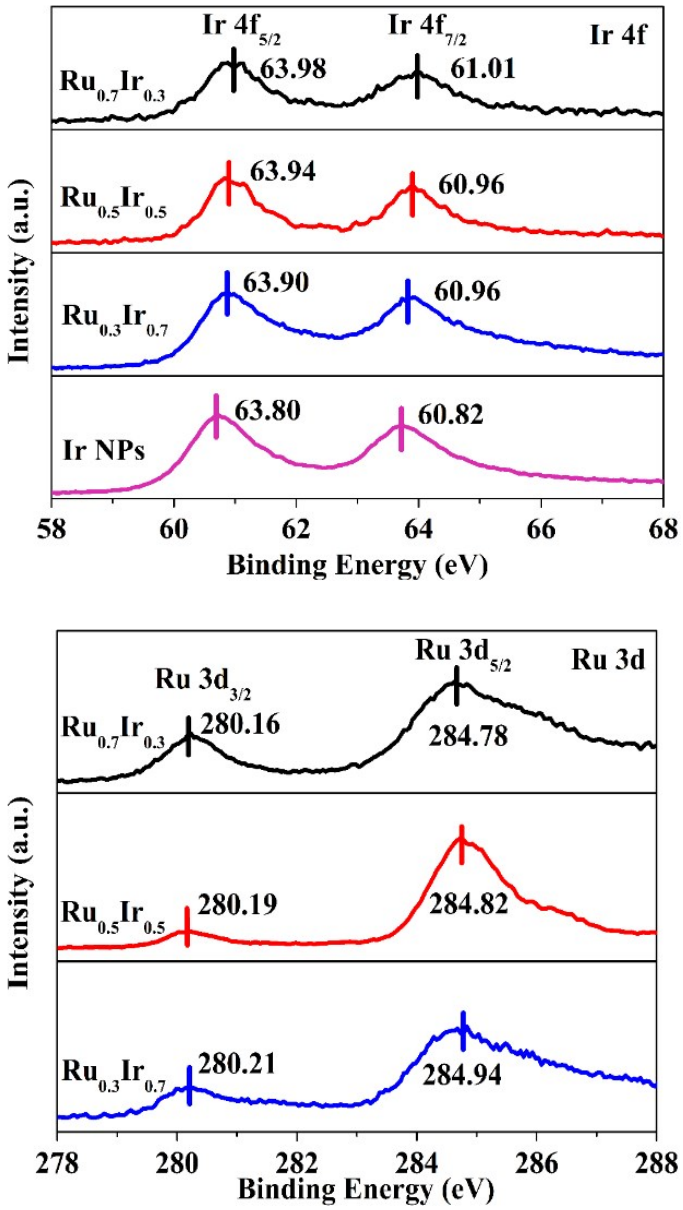

Figure S4. XPS spectra of Ir 4f and Ru 3d on Ru_xIr_{1-x} alloy NPs.

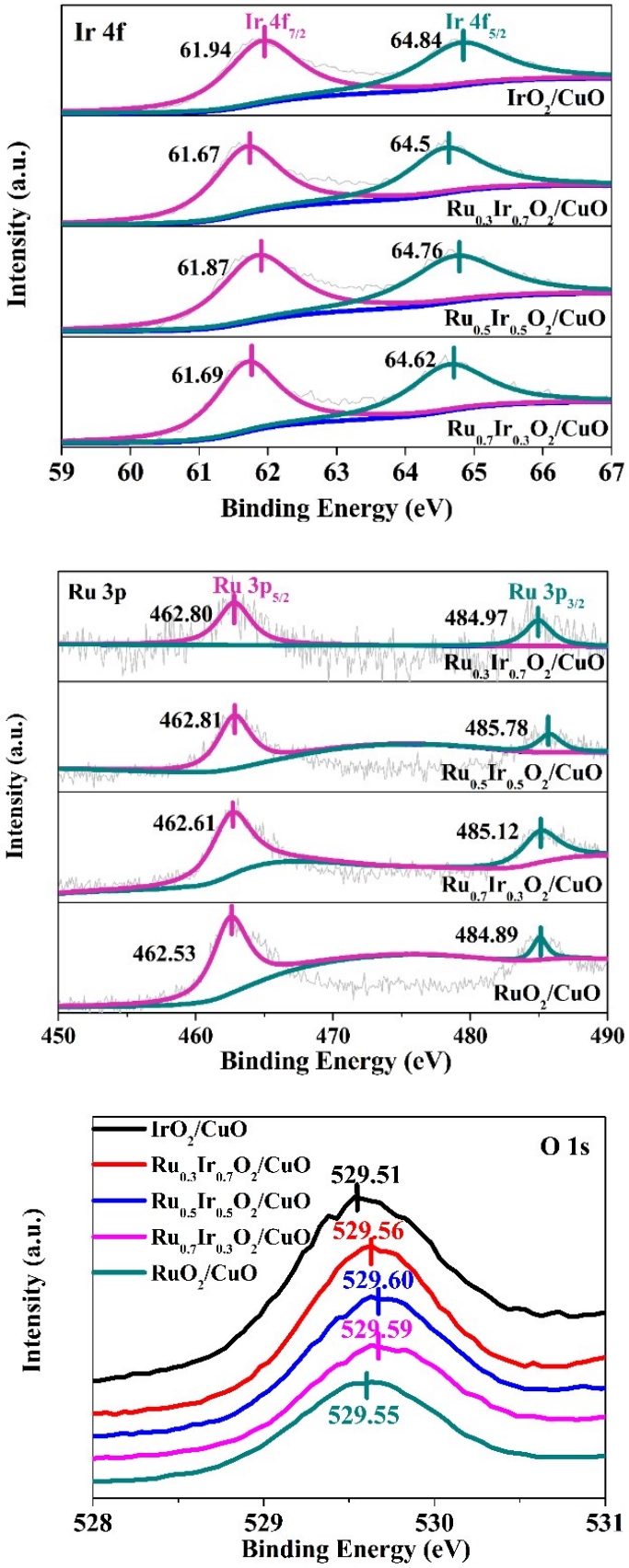

Figure S5. XPS spectra of Ir 4f, Ru 3p and O 1s on $Ru_xIr_{1-x}O_2$/CuO.

(a)

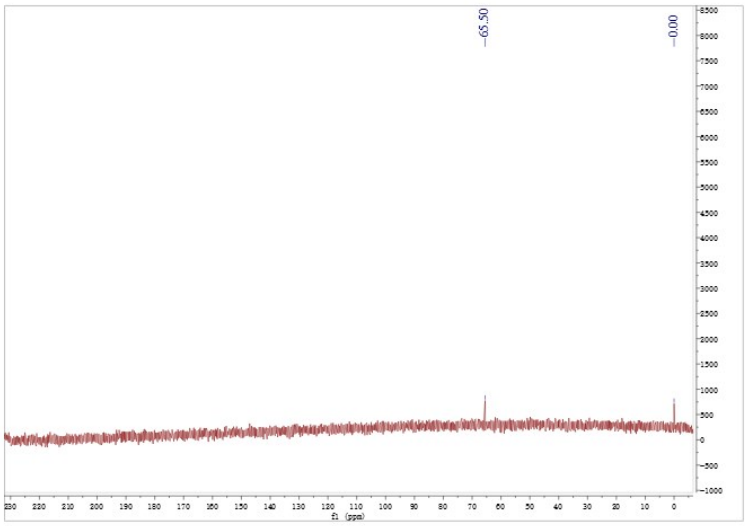

(b)

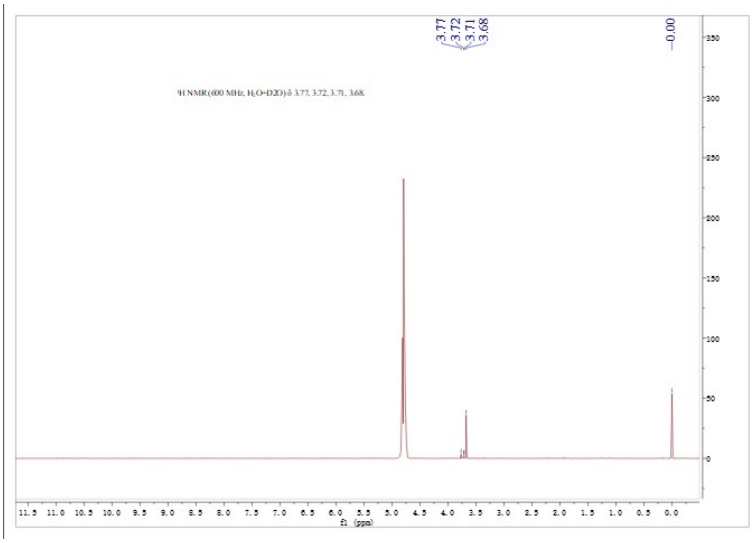

(c)

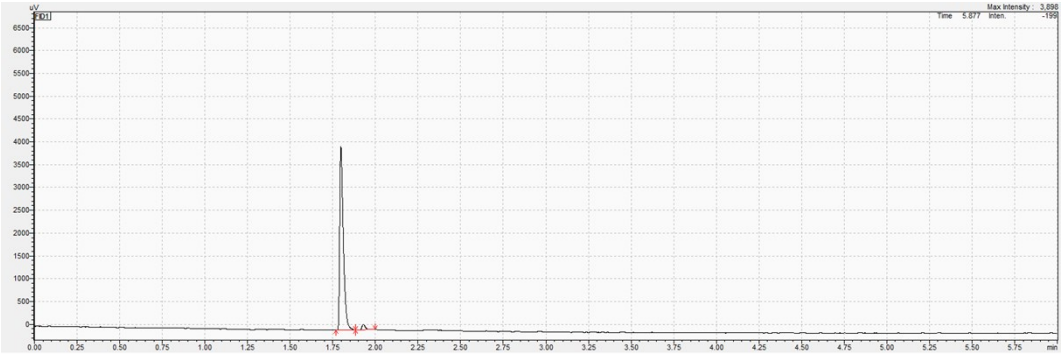

Figure S6. (a) ^{13}C NMR and (b) ^{1}H NMR spectra from reaction products. The peaks at 65.5 in ^{13}C NMR and ~3.7 in ^{1}H NMR spectra are attributed to methanol. (c) Gas chromatography of reaction products, illustrating a major product of methanol and a byproduct at the retention time of 1.81 and 1.94 min, respectively.

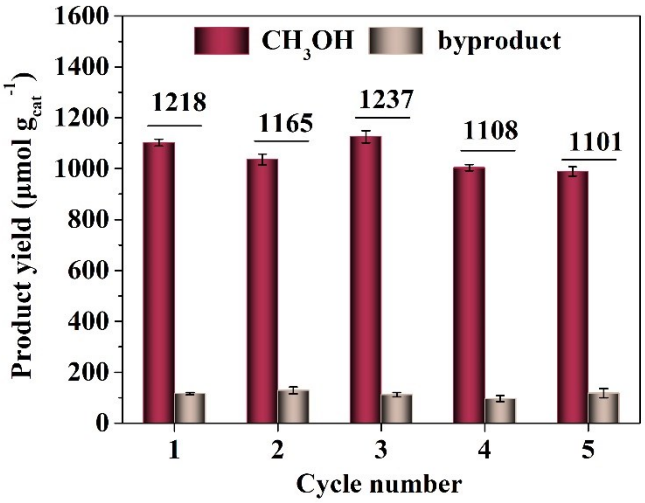

Figure S7. Stability test of methane oxidation reaction on $Ru_{0.5}Ir_{0.5}O_2$/CuO.